Deposition of fine and ultrafine aerosol particles during exposure at the air/cell interface

A. Tippe[a,*], U. Heinzmann[b], C. Roth[a]

[a]*Institute for Inhalation Biology, GSF-Research Center for Environment and Health, D-85758 Neuherberg, Munich, Germany*
[b]*Institute for Pathology, GSF-Research Center for Environment and Health, D-85758 Neuherberg, Munich, Germany*

Abstract

In vitro investigations regarding the action of aerosol particles on airway epithelial cells or alveolar macrophages are faced with the unsettled problem of controlling the number of particles deposited from the gas phase onto the cell surface (particle dosimetry). In this study we report about a new method which allows a quantitative dosimetry of fine and ultrafine aerosol particles (diameter: 75–1000 nm) during in vitro exposure of cell cultures. Combining particle transportation close to the cell surface by stagnation point flow and particle/wall contact via experimentally verified convection and the known magnitudes of Brownian diffusion and sedimentation by gravity the number of particles deposited per unit time and area of the stagnation plate could be calculated. Results of deposition experiments using fine polystyrene and ultrafine carbon black aerosol particles are in satisfactory agreement with the calculated values, indicating the utility of the proposed dosimetric method. © 2001 Elsevier Science Ltd. All rights reserved.

1. Introduction

Cell cultures prepared for in vitro studies are normally immersed in fluid culture medium either within a culture flask or within a culture dish on a supporting microporous membrane. The dosimetry of active substances then relates to the concentration of these substances in the medium (Garrett, Campbell, Stack, Waters, & Lewtas, 1981; Samet, Reed, Ghio, Devlin, Carter, Dailey, Bromberg & Madden, 1996; Becker, Soukup, Gilmour, & Devlin, 1996; Wallaert, Fahy, Tsicopoulos, Gosset, & Tonnel, 2000). However, considering in vitro investigations with

---

*Corresponding author. Tel.:+49-89-3187-2557; fax: +49-89-3187-2400.

E-mail address: tippe@gsf.de (A. Tippe).

regard to the action of aerosol particles on airway epithelial or alveolar macrophages, this in vitro design is not adequate because the physico-chemical properties of particles, cell surfaces and, therefore, particle/cell interactions change if the medium changes from a gaseous to a fluid phase. Although this problem has been recognized for a long time (Committee of the Environmental and Occupational Health Assembly of the American Thoracic Society, 1996), the corresponding in vitro experiments are predominantly performed in the presence of an overlying fluid culture medium (Goegan, Vincent, Kumarathasan, & Brook, 1998; Boland, Baeza-Squiban, Fournier, Houcine, Gendron, Chevrier, Jouvenot, Coste, Aubier, & Marano, 1999). The reasons for this unsatisfactory situation are twofold: (i) there are substantial technical difficulties to establish functional cell cultures at a gas/liquid interface and (ii) significant dosimetric problems arise if the action of aerosol particles on airway epithelial cells is to be investigated by in vitro experiments via direct access of the gas medium to the cells. To our knowledge only a few in vitro set-ups are designed to study the exposure of cells at the air/liquid interface (Voisin, Aerts, Tonnel, Houdret, & Ramon, 1975; Aufderheide & Mohr, 1999; Abe, Takizawa, Sugawara, & Kudoh, 2000). But a quantitative determination of the deposition of particles actually contacting this interface has not been discussed by these authors.

In this paper, therefore, we like to draw attention to this problem by reporting about a method which allows to determine quantitatively the number of fine or ultrafine aerosol particles deposited in the course of in vitro experiments from the gas phase at the surface of a plane cultured cell layer. The definitions of "fine" and "ultrafine" particles follow the Health Effects Institute convention which defines particles as ultrafine if the particle diameter $d < 0.1\ \mu m$, and as fine if $0.1 < d < 1.0\ \mu m$. By means of exposure experiments on glass plates using both, ultrafine carbon (count median diameter: 90 nm) and fine polystyrene particles (diameter $d = 196$ nm) the usefulness of the proposed dosimetric method could be verified.

2. General considerations

Precondition for any interaction of aerosol particles with a horizontal plate, e.g. a cell layer, is transportation towards and finally contact of the particles with the plate's surface. In case of fine and ultrafine particles, the relevant transportation mechanisms are convection by air flow, Brownian diffusion, and sedimentation by gravity. Inertial impaction can be neglected if the flow velocity u is small ($u < 1$ m/s, Schulz, Brand, & Heyder, 2000). A rotational symmetric laminar gas flow directed perpendicular to the plate's surface (stagnation point flow) was used as effective and aerodynamically simple convection mechanism for particle transportation towards a plate. Avoiding inertial impaction by slow velocities, the trajectories of fine and ultrafine particles within such flow fields follow hyperbolic streamlines which do not strike the plate but some of them will come very close to the plates surface. The final contact of the particles with the plate is then due to (1) convective transport up to a distance of r_P, the particle radius, from the plate, (2) diffusion, and (3) for larger particles (diameter $d > 200$ nm), also sedimentation. The knowledge of the hyperbolic streamline function, the mean particle displacements σ_D and σ_S in 1 s due to diffusion and sedimentation, respectively, and the particle concentration c_P [particle number/cm^3] should, therefore, be sufficient to calculate the number of particles contacting the plate during a given time interval.
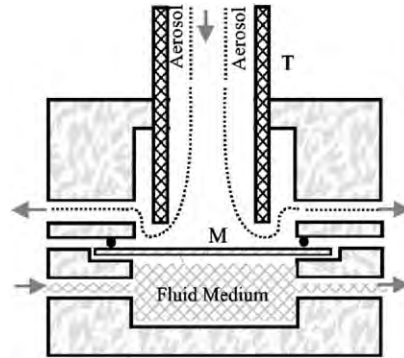
Fig. 1. Cross section of the cylindrical perfusion cell. T: inflow tube. M: membrane separating the upper and lower compartments and support of the cell layer, identical with the stagnation plate. Inner radius of the cell compartments and the inflow tube: 5 and 3 mm, respectively. Wall thickness of this tube: 1 mm. Distance of the tube end from the stagnation plate M :1 mm. The dotted lines indicate streamlines.

3. Methods

To translate these general considerations into a useful dosimetric method experiments were performed using a commercially available perfusion cell (MINUCELL, D-93077 Bad Abbach, Germany) which was reconstructed to permit an aerosol exposure by stagnation point flow (Fig. 1). In order to visualize and analyse this stagnation point flow, the upper-(aerosol) compartment of this perfusion cell was rebuilt $1:1$ using lucite as transparent material. Particle image velocimetry, PIV (Adrian, 1991), was applied to quantitatively analyse the flow field within this lucite flow cell. Briefly, the flow is visualized by means of tracer particles moving with the streaming fluid and illuminated by a sheet of laser light which is pulsed. Images of individual tracer particles are thus identified within planar sections of the 3D flow field. Due to the rotational symmetric structure of the stagnation point flow only central planes including the symmetry axis of the cell were analysed. The fluid medium was Geraniol (Haarmann & Reimer GmbH, Germany), a light oil characterized by a kinematic viscosity of $v_{oil} = 0.1 \; cm^2/s$ which is close to the air value ($v_{air} = 0.15 \; cm^2/s$). However, measured fluid velocities were corrected for by the factor $v_{air}/v_{oil} = 1.5$. Further experimental details of the PIV method used in this study are described elsewhere (Tippe, Perzl, Li, & Schulz, 1999).

As an example, Fig. 2 shows the stagnation point flow field within this cell at a Reynolds number $Re = 6.3$ ($Re = du/2v$, where d is the diameter of the inflow tube, u the mean bulk flow velocity within this tube, and v the kinematic viscosity of the fluid).

The family of streamline curves as visualized in Fig. 2 can be expressed by

$$y = 1/(a + bx),\qquad(1)$$

where a, b are linearly dependent parameters:

$$a = \alpha + \beta b\qquad(2)$$

with α, β being the numbers to be determined from the flow images. The origin of the Cartesian coordinate system x, y was placed into the left lower corner of the compartment as indicated
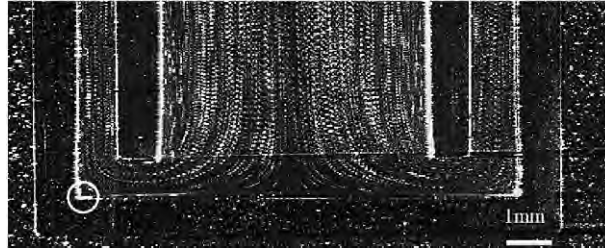
Fig. 2. Laser-light-sheet image of the stagnation point flow within the perfusion cell. Reynolds number Re = 6.3, kinematic viscosity of the fluid: $v = 0.1$ cm^2/s. The white circle in the lower left corner indicates the origine of a Cartesian x/y-coordinate system.
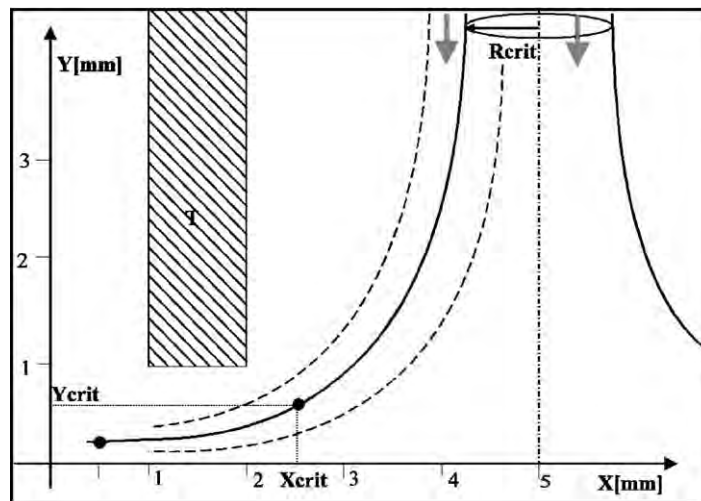
Fig. 3. Scheme of the stagnation point flow for particle deposition at the stagnation plate (X-axis). $Y_{crit} = \sigma$ and X_{crit} define a critical streamline (solid line). X_{crit} is defined by the measured particle velocity in such a way that the particle needs 1 s to move from X_{crit} to $X = 0.5$ mm along the critical streamline. R_{crit} defines the radius of the cylindrical region within the inflow which transports particles which possibly contact the plate. The Y-axis denotes the plates surface, and T, the wall of the inflow tube.

in Fig. 2. To contact the stagnation plate aerosol particles should approach this plate either by convection or to a distance which is in the order of $\sigma = \sigma_D + \sigma_S$, the mean particle displacement perpendicular to the plate, where σ_D is the root mean square displacement due to diffusion ($\sigma_D = (2Dt)^{1/2}$, D is the diffusion coefficient, and t the time) and σ_S is the displacement due to gravity. Both displacements are parallel because the deposition process creates a gradient of the particle concentration which is perpendicular to the stagnation plate. This condition defines a critical streamline and, therefore, an inner cylindrical flow region of radius R_{crit} (Fig. 3) within the inflow tube containing all those particles which possibly contact the plate.

The limitation $X = 0.5$ for the critical streamline is somewhat arbitrary but considers the fact that due to the cell geometry the stagnation streamlines became distorted in the vicinity of the outflow channel (Fig. 2). A variation of this limit between $X = 0.25$ and 0.75 mm will alter R_{crit}

by only 3%. The critical streamline, i.e. the parameters a, b from Eq. (1) can now be calculated by inserting (X_{crit}, Y_{crit}) into Eq. (1) and solving the linear system of Eqs. (1) and (2). R_{crit} then results as X-value for large Y-values, e.g. $Y = 5$ mm. As discussed in the appendix, most (more than 95%) of the aerosol particles traversing the cross section defined by R_{crit} in the inflow will be deposited onto the plate. Therefore, a practical mathematical formula for the number N_P of particles deposited within t is given by

$$N_P = 2R_{crit}^2 \pi c_P u t, \tag{3}$$

where u is the mean bulk inflow velocity, and c_P the particle concentration. Since R_{crit} is small (≈ 0.3 mm) the particle velocity within the central inflow cylinder was approximated by the maximum tube velocity: $2u$.

4. Experiments

To prove the validity of this procedure a quartz cover glass (stagnation plate) put in place of the porous membrane within the perfusion chamber was exposed to ultrafine carbon (EC-90; count median diameter: 90 nm) and fine polystyrene particles (Stadex SC-020-S, Japan Synthetic Rubber; 196 nm diameter). The deposited particles were subsequently analysed by scanning electron microscopy (SEM).

The EC-90 particles were produced by means of spark discharging (Roth, Karg, & Heyder, 1998). To get 90 nm median diameter particles the discharge frequency was set to 300 Hz. The actual particle number concentration c_P was measured several times during the exposure by means of a condensation particle counter (CPC model 3022A, TSI). As a result, an average particle concentration was determined to $c_P = 3 \times 10^6/\text{cm}^3 \pm 5\%$. The exposure time t of the quartz plate by this EC-90 aerosol within the perfusion chamber was $t = 10$ h. The aerosol flow rate was adjusted to $Q = 57$ cm^3/min $\pm 10\%$ (Re $= 6.3$; mean inflow velocity: $u = 3.15$ cm/s).

To generate the polystyrene aerosol a suspension of Stadex SC-020-S in distilled water (concentration: 1.2×10^9 per ml) was nebulized by means of a concentric stainless-steel nozzle (Schlick, Coburg, Germany) operating at an air pressure of 2×10^5 Pa, an airflow of 500 l/h in combination with a dry airflow of 500 l/h as described by Kreyling et al. (1999). These conditions led to a measured particle number concentration for the aerosol (Laser Aerosol Counter Mod. 236, Hiac/Royco) of $c_P = 1.6 \times 10^4/\text{cm}^3 \pm 20\%$. The exposure time of the quartz plate by this aerosol at a flow rate of $Q = 0.98$ cm^3/s $\pm 2\%$ was $t = 0.62$ h.

5. Results

5.1. Calculation of particle deposition

The shape of the stagnation point flow for low Reynolds numbers did not alter by varying this number between $0.5 <$ Re < 10. Based on technical grounds the actual experiments were performed at Re $= 6.3$ leading to a mean inflow velocity of $u = 3.15$ cm/s. From digital flow field images such as Fig. 2, 10 different streamlines were selected and fitted to Eq. (1). Specific parameters a, b were thus calculated (correlation coefficients $r > 0.99$). A linear fit of these

Table 1
Characteristic values of stagnation point flow parameters ($Re = 6.3$) within the perfusion chamber for different particle diameters. Critical parameters X_{crit}, Y_{crit}, and R_{crit} as defined in Fig. 3. The particle velocities $v(Y_{crit})$ are measured at a distance $Y_{crit} = \sigma$ from the stagnation plate. $\sigma = \sigma_D + \sigma_S$, σ_D and σ_S are the mean particle displacements due to diffusion and sedimentation, respectively

Particle diameter (nm)	Mean displacement $\sigma = Y_{crit}$			Particle velocity $v(Y_{crit})$ (mm/s)	X_{crit} (mm)	Critical radius R_{crit} (mm)
	σ_D (μm)	σ_s (μm)	σ (μm)			
75	50	0	50	3.70	4.20	0.30
100	39	1	40	3.00	3.50	0.32
200	22	2	24	1.70	2.20	0.34
500	12	10	22	1.50	2.00	0.33
1000	8	33	41	3.00	3.50	0.32

Table 2
Comparison of the calculated (N_P^c) and measured (N_P^m) number of deposited EC-90 and polystyrene particles per mm² of the stagnation plate

Particle	Diameter (nm)	Concentration c_P (cm^{-3})	Number of deposited particles	
			N_P^c/mm²	N_P^m/mm²
EC-90	90	$3.6 \times 10^6 \pm 5\%$	$3.1 \times 10^7 \pm 20\%$	$2.2 \times 10^7 \pm 15\%$
Polystyrene	196	$1.6 \times 10^4 \pm 20\%$	$1.1 \times 10^4 \pm 35\%$	$1.3 \times 10^4 \pm 40\%$

parameters to Eq. (2) determined the coefficients $\alpha, \beta (r = 0.998)$ to: $\alpha = -1.123$, and $\beta = -4.738$. The fluid velocity v, particularly in close vicinity to the plate ($Y < 0.2$ mm), was determined by measuring the displacement of tracer spots during a known time interval (laser pulse frequency). The values were corrected by the factor $v_{air}/v_{oil} = 1.5$ taking into account the different kinematic viscosities of fluid and air (see Section 3). Applying the software package OPTIMAS (Optimas Corp., USA) the accuracy of these measurements was about 5% (Tippe et al., 1999). For distances $Y \leqslant 0.05$ mm, the velocity was linearly extrapolated from the measured values assuming the validity of the no slip condition at the plate's surface.

Since $\sigma = \sigma_D + \sigma_S$ the mean particle displacements in 1 s are known for fine and ultrafine particles (Schulz et al., 2000), the coordinates X_{crit} and Y_{crit} and consequently R_{crit} can readily be determined for particles of different diameters. The results of these calculations are listed in Table 1. It should be emphasized that according to Table 1 the critical radius R_{crit} turned out to be almost independent from particle diameter. The average value of $R_{crit}^{av} = 0.32$ mm (with an uncertainty of about $\pm 6\%$), therefore, applies to all particles between 75 nm and 1 μm diameter. This result significantly facilitates the usage of this method, particularly in case of aerosols which are not monodisperse.

Finally, the calculated number N_P^c of particles per mm² of the stagnation plane deposited during the exposure experiment was determined according to Eq. (3). Notice that the total area of this plane was 63.6 mm². The results are listed in Table 2 together with the corresponding measured values.
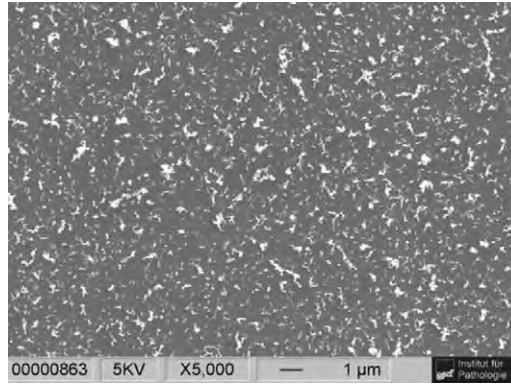
Fig. 4. Low magnification (×5000) SEM image of EC-90 particles and larger aggregates deposited during 10 h exposure within the perfusion chamber.
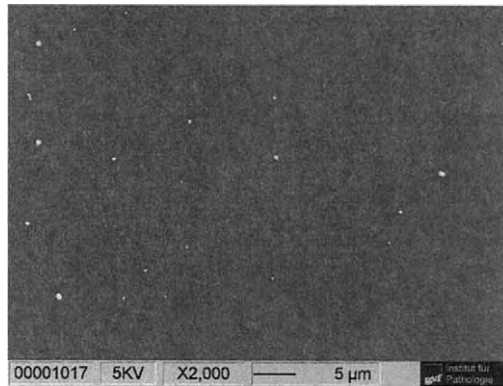
Fig. 5. Low magnification (×2000) SEM image of polystyrene particles and aggregates deposited during 0.62 h exposure within the perfusion chamber.

5.2. Measured particle deposition

Low magnification SEM images taken at different sites of the quartz plate indicated that the particles are homogeneously distributed across this plate (Figs. 4 and 5).

Examples of the specific morphology of particles and aggregates are shown at higher magnification in Figs. 6 and 7. According to these images the carbon particles are aggregates composed of a different number of small spherical primary particles (diameters are about 15 nm). To characterize EC-90 particles and determine the number of these particles deposited per unit area of the stagnation plate, SEM images ($n = 10$) from different sites at ×55.000 magnification (covering an area of 3.0 μm^2) were analysed. Single aggregates ($n = 77$) covering an area of less than 10.000 nm^2 were examined (6400 nm^2 would be covered by an idealized spherical EC-90 aggregate).

The average area of these aggregates turned out to be 5800 nm^2 (SD: 42%) which is close to the area of the idealized particle. Such particles were, therefore, considered and counted as
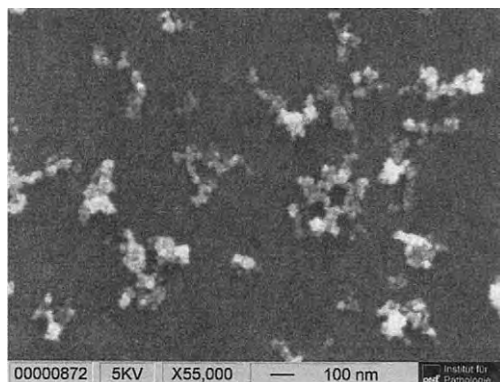
Fig. 6. SEM image of EC-90 deposited particles and aggregates at ×55.000 magnification.
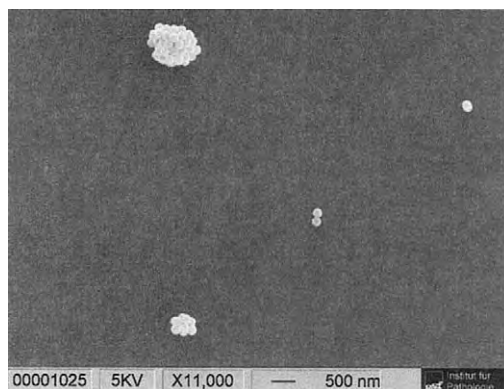
Fig. 7. SEM image of deposited polystyrene particles and aggregates at ×11.000 magnification.

single EC-90 particles. The areas of larger agglomerates were divided by the average area of single particles ($5800\,\text{nm}^2$). In a few cases EC-90 particles are overlapping. Image analysis could separate these particles by an adequate adjustment of the pixels intensity threshold. The mean particle number N deposited in an area of $3.0\,\mu\text{m}^2$ was thus determined to $N = 66 \pm 15\%$ particles/$3.0\,\mu\text{m}^2$. The measured number of particles N_P^m deposited per mm^2, therefore, was given by $N_P^m = 2.2 \times 10^7$ EC-90 particles/$\text{mm}^2 \pm 15\%$ (see Table 2).

In case of the polystyrene particles, single spheres of 196 nm diameter and different aggregates of such spheres were deposited (Fig. 7). Since the measured particle concentration c_P referred to both, single particles and particle aggregates, the number of deposited particles obtained from SEM images ($n = 10$, magnification between ×1000 and ×2000) as well did not discriminate between single and aggregated particles. The evaluation of the images resulted in a number of particles N_P^m deposited in an area of $1\,\text{mm}^2$ of $N_P^m = 1.3 \times 10^4$ polystyrene particles/$\text{mm}^2 \pm 40\%$. The results of the measured and estimated particle depositions are summarized in Table 2.

6. Discussion

In this study we examined the problem of aerosol particle deposition in the case of in vitro exposure experiments of such particles on cell cultures. For fine and ultrafine aerosol particles, a simple method was proposed and tested which permits an adjustment and quantitative control of the particle number concentration deposited on the cell surfaces during the experiments. Since in vitro experiments typically are performed using a liquid medium on both sides of the cell layer, it should be emphasized, that in accordance with deposition processes within the lung's airway system the proposed in vitro method considers particle deposition processes at an air/cell interface.

It turned out that the precise knowledge of the convective, diffusive, and gravitational particle transport towards the cell surface is essential for a successful application of the method. Whereas the diffusional and gravitational particle displacements are well-known values which can be obtained from literature, the convective transport depends upon the experimental layout. As the most simple flow field having velocity components towards a plate or a cell culture layer a rotational symmetric stagnation point flow with this layer as stagnation plate was selected. Particle image velocimetry was applied to determine the streamlines and flow velocities and, therefore, the parameters of the convective transport within this flow field. Combining diffusive, gravitational, and convective particle transport the number particle concentration N_P per unit of time and area deposited on the stagnation plate could be calculated for particle diameters between 75 nm and 1 μm. Unexpectedly, it turned out that N_P depended only on flow rate and particle concentration of the inflow aerosol but not upon particle size. This fact significantly facilitates the application of the method because it allows the treatment of polydisperse aerosols without calculating the particle deposition separately for each monodisperse fraction of the aerosol.

As indicated by the numbers listed in Table 2, there is a satisfactory agreement between the calculated and measured particle depositions. Although the numbers are within the error limits, for EC-90 particles there is a tendency to get smaller measured values when compared to calculated values. This observation agrees with the fact that the calculus implicitly assumed a 100% efficiency of deposition if the particle contacts the wall, an assumption which depends upon the particle/wall interaction and might be somewhat below the optimum for the glass surface used in the experiments. However, the difference is small and due to the moist and less plane surfaces of cell cultures compared to glass surfaces, a 100% deposition efficiency should be an adequate assumption for aerosol exposure experiments on cell cultures.

To sum up, a simple method has been proposed and successfully verified by experiments which can be considered as a practical approach to cope with the dosimetry problem of aerosol particles in the course of in vitro exposure on cultured cell layers.

Appendix

Aerosol particles traversing the spherical cross section defined by R_{crit} in the inflow tube are possible candidates for deposition onto the stagnation plate. To estimate the percentage of these

particles which in fact will be deposited, three mechanisms: convection, diffusion, and gravity will be discussed separately.

1. *Convective transport*: Aerosol particles transported along streamlines which approach the stagnation plate to a distance $Y \leqslant r_p$ (r_p is the particle radius) will contact the plates surface and, therefore, deposited onto the plate. Analogous to the definition of the critical radius R_{crit} there exists a radius $R < R_{crit}$ defining an inner spherical cross section in the inflow tube which includes all those streamlines. It turned out that for particle radius r_p between $0.035 < r_p < 0.5$ μm, R is almost constant: $R = 0.26$ mm $\pm 2\%$.

Since R_{crit} was determined to be equal to 0.32 mm, the percentage of particles deposited by convective transport amounts to 66% of all particles within the critical volume per unit time $V_{crit} = 2R_{crit}^2 \pi u$, where u is the average tube flow velocity. Otherwise, deposition by diffusion or sedimentation relates to only 34% of the particles. These particles are located in the outer part V_{DS} of V_{crit}: $V_{DS} = V_{crit} - V_c$ ($V_c = 2R^2\pi u$).

2. *Diffusion*: Due to the deposition process there is a gradient of the particle concentration perpendicular to the stagnation plate. For ultrafine particles (no sedimentation) R_{crit} was defined such that particles within V_{DS} will move for at least one second nearly parallel to the plate in a distance $Y \leqslant (2Dt)^{1/2}$, the root mean square displacement by diffusion. This flow can be compared to a laminar tube flow where aerosol particles move parallel to the tube wall in a distance $\leqslant r$, the tube radius. For this situation a mathematical solution of the deposition problem have been obtained (see Hinds, 1982). The penetration P, defined as the fraction of entering particles that exit the tube of length L, is given as

$$P = 1 - 0.819 \exp(-11.5\mu) + 0.0975 \exp(-70.1\mu) + \cdots \text{ for } \mu < 0.007$$

and

$$\mu = DL/\pi r^2 v,$$

where v is the average flow velocity within the tube ($v = L/t$). If the tube radius r and the root mean square displacement of the particles are of the same magnitude, $r = (2Dt)^{1/2}$, the flow situation within the tube with respect to deposition is comparable to that part of the stagnation point flow in the perfusion cell where streamlines within V_{DS} are almost parallel to the stagnation plate. In this case:

$$\mu = 1/2\pi$$

and,

$$P = 0.13.$$

This result signifies that 87% of the incoming aerosol particles will be deposited onto the walls within the tube, or 87% of the ultrafine particles within V_{DS} are deposited onto the stagnation plate. Together with the particles deposited by convection the fraction of ultrafine particles within V_{crit} deposited onto the plate amounts to more than 95%.

3. *Sedimentation*: As shown in Table 1, particle displacement towards the stagnation plate caused by gravity increases with increasing particle size whereas displacement by diffusion

decreases. Considering aerosol particles of 1 μm diameter the settling velocity is about 33 μm/s. Compared to at most 40 μm distance between the stagnation plate and particles moving at least 1 s along the horizontal part of the critical streamline, this settling velocity causes about 83% of the 1 μm particles within V_{DS} to be deposited onto the plate. Therefore, the fraction of 1 μm (fine) particles within V_{crit} deposited by convection and gravity onto the plate amounts to about 95%. For particles of intermediate size (0.075–1 μm) the fraction of particles deposited by convection, diffusion, and gravity will be in the same order of magnitude, $\geqslant$ 95%.

This result justifies the assumption made in this study that the cylindrical volume V_{crit} within the inflow contains those fine and ultrafine aerosol particles which will be deposited onto the stagnation plate, as the error introduced by this assumption ($<$ 5%) is small compared to the measuring errors discussed above (Section 5) and summarized in Table 2.

References

Abe, S., Takizawa, H., Sugawara, I., & Kudoh, S. (2000). Diesel exhaust (DE)-induced cytokine expression in human bronchial epithelial cells. *American Journal of Respiration and Cell Molecular Biology*, *22*, 296–303.

Adrian, R. J. (1991). Particle-imaging techniques for experimental fluid mechanics. *Annual Review of Fluid Mechanics*, *23*, 261–304.

Aufderheide, M., & Mohr, U. (1999). CULTEX—A new system and technique for the cultivation and exposure of cells at the air/liquid interface. *Experiments in Toxicology and Pathology*, *51*, 489–490.

Committee of the Environmental and Occupational Health Assembly of the American Thoracic Society., (1996) Health effects of outdoor air pollution. Part 1. *American Journal of Respiration and Critical Care Medicine*, *153*, 3–50.

Becker, S., Soukup, J. M., Gilmour, M. I., & Devlin, R. B. (1996). Stimulation of human and rat alveolar macrophages by urban air particulates: Effects on oxidant radical generation and cytokine production. *Toxicology and Applied Pharmacology*, *141*, 637–648.

Boland, S., Baeza-Squiban, A., Fournier, T., Houcine, O., Gendron, M.-C., Chevrier, M., Jouvenot, G., Coste, A., Aubier, M., & Marano, F. (1999). Diesel exhaust particles are taken up by human airway epithelial cells in vitro and alter cytokine production. *American Journal of Physiology* (*Lung Cellular and Molecular Physiology, 20*), *276*, L604.

Garrett, N. E., Campbell, J. A., Stack, H. F., Waters, M. D., & Lewtas, J. (1981). The utilization of the rabbit alveolar macrophage and chinese hamster ovary cell for evaluation of the toxicity of particulate materials. *Environmental Research*, *24*, 345–365.

Goegan, P., Vincent, R., Kumarathasan, P., & Brook, J. (1998). Sequential in vitro effects in lung macrophages and reporter CAT-gene cell lines. *Toxicology In Vitro*, *12*, 25–37.

Hinds, W. C. (1982). Brownian motion and diffusion. *Aerosol Technology* (pp. 133–152). New York: Wiley.

Kreyling, W. G., Blanchard, J. D., Godleski, J. J., Haeussermann, S., Heyder, J., Hutzler, P., Schulz, H., Sweeney, T. D., Takenaka, S., & Ziesenis, A. (1999). Anatomic localization of 24- and 96-h particle retention in canine airways. *Journal of Applied Physiology*, *87*, 269–284.

Roth, C., Karg, E., & Heyder, J. (1998). Do inhaled ultrafine particles cause acute health effects in rats? I: Particle production. *Journal of Aerosol Science*, *29*, S679–S680.

Samet, J. M., Reed, W., Ghio, A. J., Devlin, R. B., Carter, J. D., Dailey, L. A., Bromberg, P. A., & Madden, M. C. (1996). Induction of prostaglandin H synthase 2 in human airway epithelial cells exposed to residual oil fly ash. *Toxicology and Applied Pharmacology*, *141*, 159–168.

Schulz, H., Brand, P., & Heyder, J. (2000). Particle deposition in the respiratory tract. In P. Gehr, & J. Heyder (Eds.), *Lung biology in health and diseases*, *particle–lung interaction* Vol. 143 (pp. 229–290). New York: Marcel Dekker.

Tippe, A., Perzl, M., Li, W., & Schulz, H. (1999). Experimental analysis of flow calculations based on HRCT imaging of individual bifurcations. *Respiration Physiology*, *117*, 181–191.

Voisin, C., Aerts, C., Tonnel, A. B., Houdret, L. J., & Ramon, P. (1975). Mise en survie en phase gazeuse et reconstitution in vitro du microenvironnement naturel des macrophages alveolaires. *Pathologie et Biologie*, *23*, 453–461.

Wallaert, B., Fahy, O., Tsicopoulos, A., Gosset, Ph., & Tonnel, A. B. (2000). Experimental systems for mechanistic studies of toxicant induced lung inflammation. *Toxicology Letters*, *112–113*, 157–163.